SINTEF
PROCEEDINGS
1

Selected papers from 10th International Conference on Computational Fluid Dynamics in the Oil & Gas, Metallurgical and Process Industries

Progress in Applied CFD

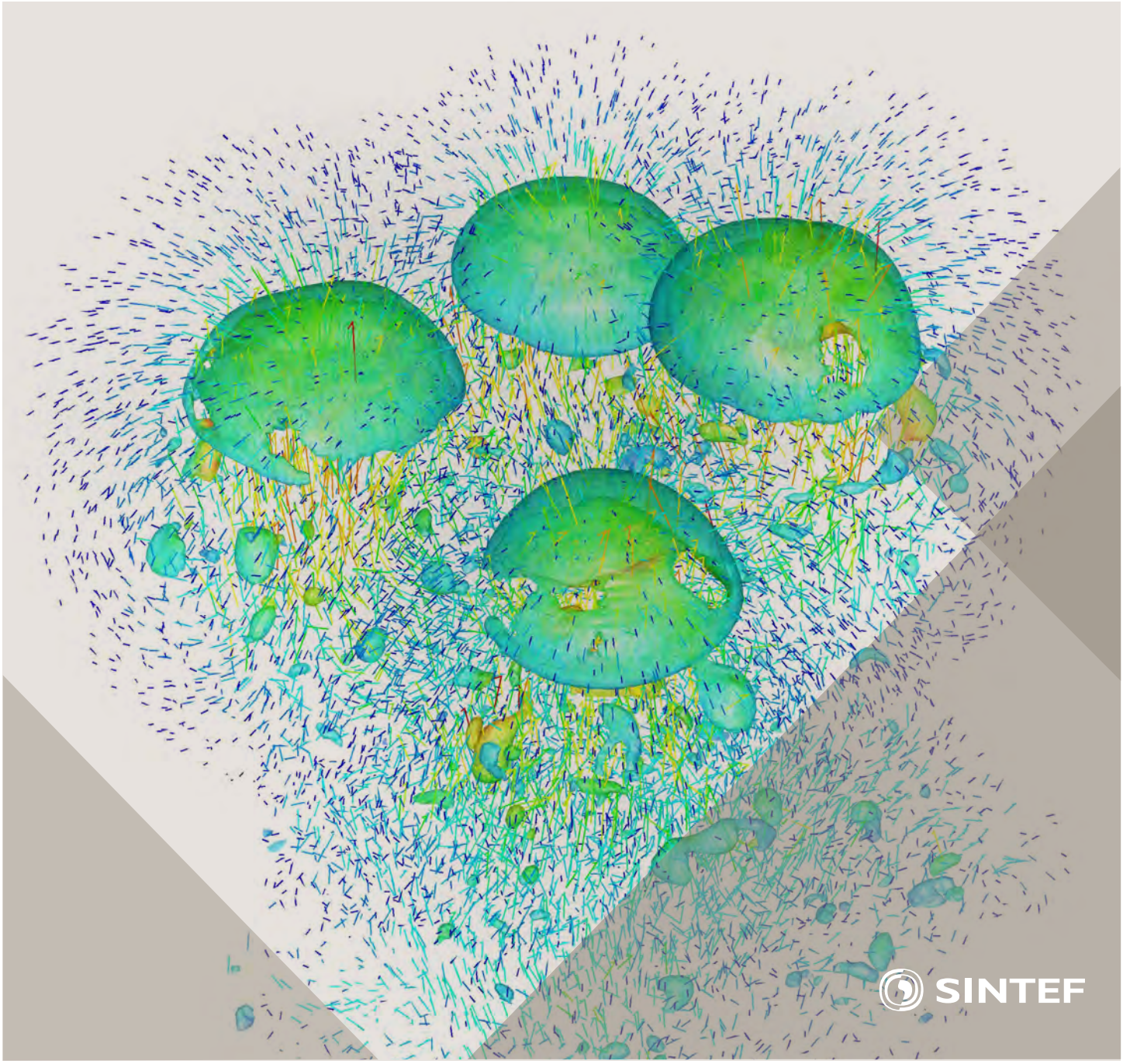

SINTEF Proceedings

Editors:
Jan Erik Olsen and Stein Tore Johansen

Progress in Applied CFD

Selected papers from 10th International Conference on Computational Fluid Dynamics in the Oil & Gas, Metallurgical and Process Industries

SINTEF Academic Press

SINTEF Proceedings no 1
Editors: Jan Erik Olsen and Stein Tore Johansen
Progress in Applied CFD
Selected papers from 10th International Conference on Computational Fluid Dynamics in the Oil & Gas, Metallurgical and Process Industries

Key words:
CFD, Flow, Modelling

Cover, illustration: Rising bubbles by Schalk Cloete

ISSN 2387-4287 (printed)
ISSN 2387-4295 (online)
ISBN 978-82-536-1432-8 (printed)
ISBN 978-82-536-1433-5 (pdf)

60 copies printed by AIT AS e-dit
Content: 100 g munken polar
Cover: 240 g trucard

SINTEF Academic Press
Address: Forskningsveien 3 B
PO Box 124 Blindern
N-0314 OSLO
Tel: +47 22 96 55 55
Fax: +47 22 96 55 08

www.sintef.no/byggforsk
www.sintefbok.no

SINTEF Proceedings
SINTEF Proceedings is a serial publication for peer-reviewed conference proceedings on a variety of scientific topics.
The processes of peer-reviewing of papers published in SINTEF Proceedings are administered by the conference organizers and proceedings editors. Detailed procedures will vary according to custom and practice in each scientific community.

PREFACE

This book contains selected papers from the 10th International Conference on Computational Fluid Dynamics in the Oil & Gas, Metallurgical and Process Industries. The conference was hosted by SINTEF in Trondheim in June 2014 and is also known as CFD2014 for short. The conference series was initiated by CSIRO and Phil Schwarz in 1997. So far the conference has been alternating between CSIRO in Melbourne and SINTEF in Trondheim. The conferences focus on the application of CFD in the oil and gas industries, metal production, mineral processing, power generation, chemicals and other process industries. The papers in the conference proceedings and this book demonstrate the current progress in applied CFD.

The conference papers undergo a review process involving two experts. Only papers accepted by the reviewers are presented in the conference proceedings. More than 100 papers were presented at the conference. Of these papers, 27 were chosen for this book and reviewed once more before being approved. These are well received papers fitting the scope of the book which has a slightly more focused scope than the conference. As many other good papers were presented at the conference, the interested reader is also encouraged to study the proceedings of the conference.

The organizing committee would like to thank everyone who has helped with paper review, those who promoted the conference and all authors who have submitted scientific contributions. We are also grateful for the support from the conference sponsors: FACE (the multiphase flow assurance centre), Total, ANSYS, CD-Adapco, Ascomp, Statoil and Elkem.

Stein Tore Johansen & Jan Erik Olsen

Organizing committee:

Conference chairman: Prof. Stein Tore Johansen
Conference coordinator: Dr. Jan Erik Olsen
Dr. Kristian Etienne Einarsrud
Dr. Shahriar Amini
Dr. Ernst Meese
Dr. Paal Skjetne
Dr. Martin Larsson
Dr. Peter Witt, CSIRO

Scientific committee:

J.A.M.Kuipers, TU Eindhoven
Olivier Simonin, IMFT/INP Toulouse
Akio Tomiyama, Kobe University
Sanjoy Banerjee, City College of New York
Phil Schwarz, CSIRO
Harald Laux, Osram
Josip Zoric, SINTEF
Jos Derksen, University of Aberdeen
Dieter Bothe, TU Darmstadt
Dmitry Eskin, Schlumberger
Djamel Lakehal, ASCOMP
Pär Jonsson, KTH
Ruben Shulkes, Statoil
Chris Thompson, Cranfield University
Jinghai Li, Chinese Academy of Science
Stefan Pirker, Johannes Kepler Univ.
Bernhard Müller, NTNU
Stein Tore Johansen, SINTEF
Markus Braun, ANSYS

CONTENTS

COOL-DOWN SIMULATIONS OF SUBSEA EQUIPMENT

Atle JENSEN[12*], Stig GRAFSRØNNINGEN[1]
[1] FMC Technologies, 1386 Asker, NORWAY
[2] Dep. of mathematics, Univ. of Oslo, 0316 Oslo, NORWAY
* E-mail: atle.jensen@fmcti.com

ABSTRACT

Experiments and numerical conjugate heat transfer simulations are performed on a simple T-pipe geometry. The T-pipe geometry is partially insulated and mimics subsea equipment which is subject to cool-down after a production shut-down. During flowing conditions the flow is turbulent before closing down and cool-down starts. After some time after shut-down the flow becomes near stagnant in parts of the geometry whereas it remains turbulent in the vertical section for a long time after shut-down due to large buoyant forces. Velocities were measured with particle image velocimetry (PIV), whereas temperature was measured using resistance temperature detectors (RTD's) and thermocouples. A particular focus is on the effect of using Reynolds-averaged Navier–Stokes (RANS) turbulence models on a buoyant flow which is laminar, transitional and turbulent within a single fluid domain.

Keywords: CFD, turbulence, natural convection, PIV.

NOMENCLATURE

Greek Symbols
ρ Mass density, [kg/m^3].
μ Dynamic viscosity, [kg/ms].
ν Kinematic viscosity, [m^2/s].
β Coefficient of thermal expansion, [1/K].
α Thermal diffusivity, [m^2/s].
σ Stefan-Boltzmann constant, [W/m^{2}K^4].
ε Emissivity, [-].
ε Turbulent dissipation rate, [m^2/s^3].
δ Kronceker Delta, [-].
ω Turbulence eddy frequency, [1/s].

Latin Symbols
L Characteristic length, [m].
p Pressure, [Pa].
u Velocity, [m/s].
g Gravitational acceleration [m/s^2].
h Heat transfer coefficient [W/m^{2}K].
k Thermal conductivity, [W/mK].
k Turbulent kinetic energy [m^2/s^2].
T Temperature, [°C].

Sub/superscripts
G Gas.
i Index i – spatial direction x.
j Index j – spatial direction y.
s Surface.
∞ Ambient.
t Turbulent.

INTRODUCTION

In subsea oil and gas industry, thermal insulation of equipment is often used as a method to slow down cool-down, and to facilitate shut-down procedures. Great effort is spent on predicting the thermal behaviour of hydrocarbon production systems in order to identify and prevent hydrate formation in the production fluid during normal production, and during planned or unplanned shut downs.

Subsea equipment generally cannot be fully insulated for different reasons; avoid overheating of electronic components, facilitate remotely operated underwater vehicle (ROV) access, clearance, and various other reasons. The uninsulated parts of the subsea equipment create cold-spots which may have a severe effect on the thermal performance. Detailed thermal analyses are required to assess the effect of these cold-spots and to make sure the equipment is adequately insulated. An increasingly large fraction of the detailed thermal analyses within the subsea industry nowadays are conjugate heat transfer computational fluid dynamics (CFD) simulations.

Engineering flows are generally turbulent and laminar flows are seldom encountered. One exception is natural convection, i.e. buoyancy driven flow. During cool-down of subsea equipment, laminar, transitional and turbulent flow may occur simultaneously within the same domain. RANS-turbulence models, which is the only feasible level of turbulence treatment in CFD for engineering purposes on full scale equipment, are developed for high Reynolds number flow and are generally unable to predict the correct solution if the actual flow is laminar or transitional.

CFD simulations are often used in the design process of the insulation on subsea equipment in the subsea industry. However, the accuracy and uncertainty of the

simulations are seldom reported, nor are the results verified against experimental data. The use of mainstay engineering CFD approaches introduces an uncertainty due to the inadequacy of the RANS-models to capture laminar to turbulent transitions and relaminarizations.

An assessment of the effect of using turbulence models on such transitional flows has been performed in order to shed some light on the uncertainty of thermal CFD cool-down simulations.

Only a few papers have investigated the thermal performance of straight vertical or horizontal dead legs in order to understand the convective behavior of the fluid. Habib et al. (2005) conducted an experimental and numerical study of the effect of dead leg geometry and average flow velocity on oil/water separation in dead legs. The length of the dead leg was varied and a fluid mix of 90% oil and 10% water was considered. They concluded that the size of the stagnant fluid region increased with increased length to diameter ratio and decreased with increased inlet velocity. Asteriadou et al. (2009) presents several CFD models of a flow in a T-piece configuration. The computational models were validated by experiments. The flows varied from laminar to turbulent. The authors report that finer mesh and enhanced wall functions application with mesh refinement did not seem to have a positive impact on the solution.

A handful of papers were found on cool-down, numerical modelling and experiments. Taxy and Lebreton (2004) conducted CFD simulations and full scale insulation tests. They concluded that numerical simulations helped to understand the phenomenology observed during different tests and were the key element to determine the correct action to implement in the insulation design. In Moe et al. (2005) the temperature development in two simple geometries and one gate valve were tested in a laboratory and analyzed with CFD. They found excellent agreement in some of the cases and concluded that CFD is a suitable tool for cool-down simulations. Furthermore, they also claimed that CFD would provide valuable input to finite element analysis (FEA) simulations to correct for the convective heat transfer. A full scale cool-down test of an X-Tree was used to verify the design and numerical models in Aarnes et al. (2005). CFD and FEA agreed very well with the test results in the main part of the X-Tree system.

Mme et al. (2008) presented results from both experiments and numerical modeling of a cool-down in a pipe with a cold spot. The inclination of the pipe was varied and it was found that the heat transfer was most efficient when the inclination was close to horizontal. CFD with a k-ε model was used to simulate the cool-down. The heat flow by the simulations was reported to be under-predicted up to 25%. In a recent paper by Lu et al. (2011), CFD and FEA were validated against controlled experiments. A coated 24 inch steel pipe was welded onto a production tree and elbow. The test assembly was placed in fresh water and temperatures were measured with thermocouples. Measurements were conducted in steady-state and during cool-down. The discrepancy was 5% between CFD and experiments for both cases. FEA gave similar results compared to the experiments.

This article presents results from conjugate heat transfer cool-down CFD simulations with comparison against cool-down experiments with a particular focus on the effect of using RANS turbulence-models on a buoyant flow which is laminar, transitional, and turbulent, within a single fluid domain.

EXPERIMENTS

For validation of the CFD model, experiments were conducted at the Hydrodynamics laboratory, University of Oslo. An idealized geometry in transparent material (Plexiglass) was chosen to give access to optical measurement techniques but also the possibility for more quantitative analysis, e.g. observations.

Experimental setup and techniques

A large diameter (ID 6") horizontal pipe (3m long header) with a vertical branch (1m) mounted together was used in the experiments (shown in Figures 1 and 2). The vertical dead-leg must be long to be able to generate flow with Rayleigh numbers ($Ra = \frac{g\beta\Delta TL^3}{\nu\alpha}$) encountered in subsea equipment. The characteristic length scale used in the Rayleigh number is the free vertical length, i.e. the length of the dead-leg in the dead-leg, and the diameter in the header region.

Water was used as test media and circulated until the required temperature was met and steady state conditions were reached (stage 1 - steady state). The flow rate was 1300 kg/h with an accuracy of +/- 0.5%. The inlet temperature was 45°C and the ambient temperature was 21°C.

A set of valves were mounted on each side of the test rig to be able to enclose the flow (state 2 - cool-down). The header was insulated with Glava (40mm) and installed horizontally on a table covered with Styrofoam to avoid heat transfer to and from the table.

Fluid velocities and external/internal temperatures were measured with high accuracy using PIV, flow meters, PT100 RTD sensors and thermocouples. PIV has seen an increase in popularity over the last two decades, much caused by the developments in camera and laser technology. This method is using pattern matching techniques to be able to track the motion of passive particles which are added to the flow. A sequence of images is used in the post-processing to find the temporal variation of the velocity in a flow. Kinematics and dynamics can be found using various processing techniques. The PT100 sensors were measuring the water temperature, whereas the thermocouples were measuring the wall temperature at different positions in the interior and exterior. The accuracy of PIV is very high if the experiments are carefully executed, the error is expected to be around 1%.

The vertical pipe (dead-leg) is not insulated, thus, from a modeling point of view, the external boundary conditions between the pipe geometry and the air (a heat transfer coefficient in conjunction with an ambient temperature and the radiative heat loss) is very important. Contradictory to for fully insulated equipment the value of the heat transfer coefficient will potentially influence the results to a great extent. However, the header is insulated to be able to simulate more realistic subsea conditions, i.e. equipment which is partially insulated.

During stage 2 (cool-down) the internal and external temperatures were measured together with velocity fields. The temperatures were sampled continuously, but the velocity fields were acquired every five minutes. The velocity field results presented herein is the average of several experiments.

Water temperature was measured at 7 different locations using RTD's inserted 50 mm into the header and dead-leg. The locations of the sensor locations/measuring points are listed in Table 1. The location of the RTD's can also be seen in Figure 1 and a different view with coordinate system in Figure 2.

Table 1: Internal sensor locations.

Sensor name	Location		
	X [m]	Y [m]	Z [m]
PT1	0	0.0225	-0.977
PT2	0	0.0225	-0.377
PT3	0	0.0225	0.396
PT4	0	0.0225	0.996
PT5	0	0.397	0.023
PT6	0	0.797	0.023
PT7	-0.059	0.950	0

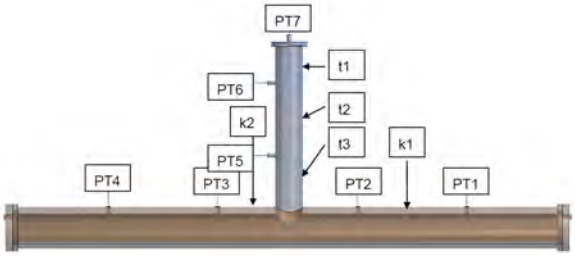

Figure 1: Side view of CFD-model with insulation and sensor locations.

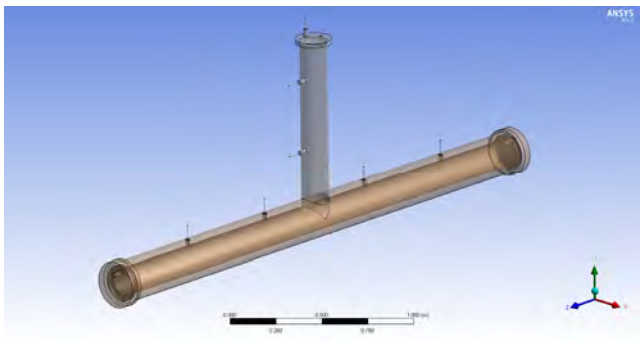

Figure 2: Perspective view showing the orientation of the coordinate system.

Type-t and type-k thermocouples were used to measure the external temperature of the test-geometry. For redundancy three sensors were used to measure the external temperatures at each location. The results from these sensors are not presented.

CFD SIMULATIONS

A side view of a CFD-model of the experimental setup is shown in Figure 1. The model contains the Plexiglas geometry, the insulation, and sensors. The RTD's used to measure the internal fluid temperatures are large and intrusive and may influence the results if not accounted for. Hence, a simplified version of the sensor was included in the CFD-model. The simulations were run using ANSYS CFX v.14.5.

The CFD-simulations were run in two stages; the first to mimic the production phase in a subsea system, i.e. flow through the geometry before a planned or unplanned shut-down. The second stage emulates the shut-down phase, i.e. from the initial valve closure and the subsequent cool-down. The second stage uses the results from the first stage as an initial condition.

The heat transfer from the test geometry to the ambient air is governed by radiation and convection. The radiative heat transfer was modeled assuming black body radiation, i.e. the heat loss due to radiation is modeled as

$$q_{rad} = \epsilon\sigma({T_s}^4 - {T_\infty}^4) \quad (1)$$

where ε is the emissivity of the body, σ is the Stefan-Boltzmann constant, T_s is the surface temperature, and T_∞ is the ambient temperature. The external Nusselt number ($Nu = \frac{hL}{k}$) due to convective heat transfer on the dead-leg was computed using the following empirical correlation

$$\overline{Nu} = [0.825 + \frac{0.387Ra^{1/6}}{[1+(\frac{0.492}{\mathrm{Pr}})^{9/16}]^{8/27}}]^2 \quad (2)$$

, where $Pr = \frac{\nu}{\alpha}$ (Prandtl number). This equation is valid for vertical walls, and vertical cylinders under certain conditions. A similar correlation (other constants) was used to compute the Nusselt number for the header, see Incropera (2007).

During stage 1 the flow in the geometry is a combination of forced, mixed and natural convection. The flow in the header is dominated by forced convection, whereas both forced and natural convection is of importance in the lower part of the dead-leg. In the upper part of the dead-leg natural convection is of sole importance. Similar effects are expected for actual subsea equipment as well.

During stage 2, after the circulation has stopped and the isolation valves are closed, a convective pattern inside the geometry develops due to the thermal differences in the system. The level of mixing in the header during stage 1 and stage 2 depends on the flow pattern. If the flow is turbulent, the mixing between the header and dead-leg regions is large whereas it is limited if the flow is laminar. Whether a flow is laminar or turbulent is given by local conditions.

Turbulence is generated by mean velocity shear and coupled turbulent velocity and temperature fluctuations, whereas it is suppressed by thermal stratifications and turbulent shear. Mean shear dominates production of turbulent kinetic energy, hence for a vertical pipe, given that the Rayleigh number is large enough, the turbulence will be generated in the shear region close to the wall. For intermediate Rayleigh numbers such a configuration may lead to intermittent flow, where intermittent alludes to a flow which spatially and temporally is turbulent.

Simulations with different turbulence models were conducted to determine the effect of the various RANS turbulence models;

- *k-ω*
  - Two-equation model – first moment closure model
- *SST*
  - Two-equation model – first moment closure model
- *RSM-ω*
  - Reynolds Stress model – second moment closure model
- *k-ε*
  - Two-equation model – first moment closure model

Historically the *k-ε* model has been the mainstay turbulence model within engineering, and still is within some communities. Turbulence models are generally developed based on assumptions of high Reynolds number flow, which does not fit the nature of turbulent natural convection flow very well.
The near wall mesh in turbulent simulations is generally very important to accurately calculate the wall shear and heat fluxes. RANS-models often use wall functions to predict the near wall physics as the near wall mesh requirements may become prohibitively stringent for high Reynolds number flow. The wall functions use models to account for the near wall physics without having to resolve the innermost region of the boundary layer with the computational grid. Wall functions are based on functions which describe the viscous sub-layer and the buffer layer found in high Reynolds number flow. However, the near wall physics found in turbulent natural convection does not resemble that of the forced flow; hence wall functions cannot be used to accurately predict turbulent natural convection.

Some of the turbulence models available in CFX (*ω*-based models, both single moment and second moment closures) and other CFD-packages use a low-Reynolds number formulation in innermost part of the boundary layer. In order to exploit the low-Reynolds number formulation a near wall mesh resolution of $y^+ < 1$ is required to avoid the use of wall functions.

The *ε*-based turbulence models, both first moment closures and second moment closures generally rely on wall functions even though the near wall mesh is $y^+ < 1$. It should be noted that it is generally recommended to avoid very fine near wall mesh resolutions ($y^+ > 30$) when using the *k-ε* model as this combination is known to produce strange results. A $y^+ > 30$ cannot be guaranteed even for rather coarse near wall meshes for such geometries due to near stagnant flow in some regions. The *ε*-based turbulence models do not switch to a low-Reynolds number formulation close to walls for fine meshes. This makes the *ε*-based turbulence models unsuited for turbulent natural convection flows. A simulation using the widely used *k-ε* model is included to assess the effect of using this model even though it is anticipated that the results are poor. The results observed herein for the *k-ε* model may to a certain extent be attributed to a too fine near wall mesh.

Barakos and Mitsoulis (1994) investigated natural convection in a square cavity for a wide range of Rayleigh numbers numerically using turbulence models with and without wall functions. Their results show that the predicted Nusselt number deviates significantly from the experimental data when wall functions are used. The predicted Nusselt number is twice that of the experimental data for large Rayleigh numbers, whereas results from simulations without wall functions compare well with the experimental data.

The *k-ω* turbulence model is known to produce good results for natural convection in enclosures and lid-driven cavities. However, all the single moment closures use a single scalar to describe the turbulence which leads to the inherent assumption that the turbulence is isotropic, which for buoyant turbulent flows is not the case. Furthermore, the single moment closures rely on the Boussinesq-approximation to relate Reynolds stresses to the mean shear $-\overline{u_i u_j} = 2\nu_t S_{ij} - 2/3k\delta_{ij}$. Here $\overline{u_i u_j}$ is Reynolds stresses, ν_t is turbulent eddy viscosity, S_{ij} is the rate of strain tensor, and k is turbulent kinetic energy. This assumption leads further to an inherent equilibrium between the Reynolds stresses and mean shear, which is generally not valid for buoyant turbulent flows. Nevertheless, even though single moment closures does not have the best prerequisites to accurately model this type of flow, simulations using single moment closure models are

included here to see if they are able to produce adequate results or not.

Simulations with three different meshes using the *k-ω* model were conducted to determine which mesh level that was required to obtain mesh independent results. All meshes were made of a combination of tetrahedrons, hexagons and prisms. Conformal mesh was used for nearly the entire model. On curved interphases such as for the inner pipe wall it is important to use a conformal mesh. If a non-conformal mesh is used it is vital that the mesh resolution is fine enough so that the surface area on both sides of the interphase is accurately predicted. On the interphase the heat flux is conserved, if the surface area on each side of the interphase is different, the heat flux will not be conserved. A non-conformal coarse surface (interphase) mesh may significantly influence the results in a conjugate heat transfer simulation. Sweep mesh was used on the piping where possible. The mesh in a part of the geometry is shown in Figure 3.

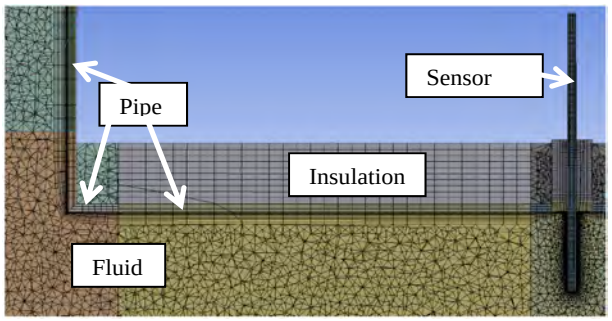

Figure 3: Fine mesh - note that the domains have been decomposed to ease the meshing process, hence the same domain may have different colors in this figure.

Key mesh sizes for the coarse, intermediate, and fine mesh are listed in Table 2.

Table 2: Mesh sizes

	Coarse	Intermediate	Fine
Total number of nodes	0.42M	1.10M	1.54M
Radial cell count insulation	2	6	10
Radial cell count uninsulated piping	2	5	8
Radial cell count insulated piping	2	3	5
Circumferential cell count on piping	40	40	60
First layer height piping	2e-3 [m]	2e-4 [m]	2e-4 [m]
Number of layers piping	7	12	12
Body sizing on piping (where applicable)	5e-3 [m]	5e-3 [m]	4e-3 [m]
Body sizing on insulation (where applicable)	1e-2 [m]	5e-3 [m]	5e-3 [m]
Body sizing on fluid	1.5e-2 [m]	7e-3 [m]	7e-3 [m]

The mesh convergence tests showed that the intermediate and fine mesh produced near identical results, but that there were minor differences, hence the fine mesh was used for the rest of the simulations. Results from the mesh convergence test are shown in Figure 4 and Figure 5. Note that the difference in internal temperature between the intermediate and fine mesh hardly is discernible here. The differences in internal wall temperatures were larger. The wall temperatures in the dead-leg (both internally and externally) for the intermediate and fine mesh differed to some extent, hence it is concluded that the fine mesh is required (results not shown here).

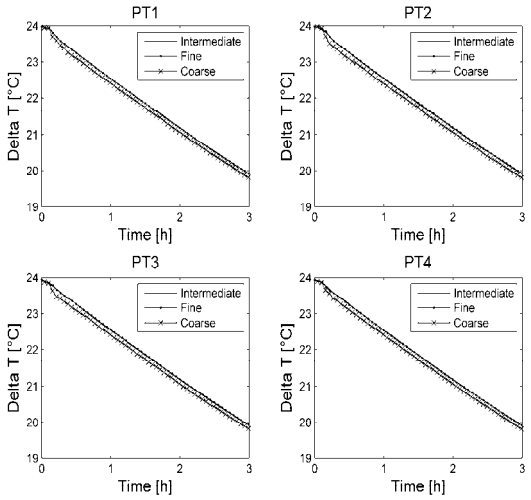

Figure 4: Mesh convergence - temperature data during cool-down

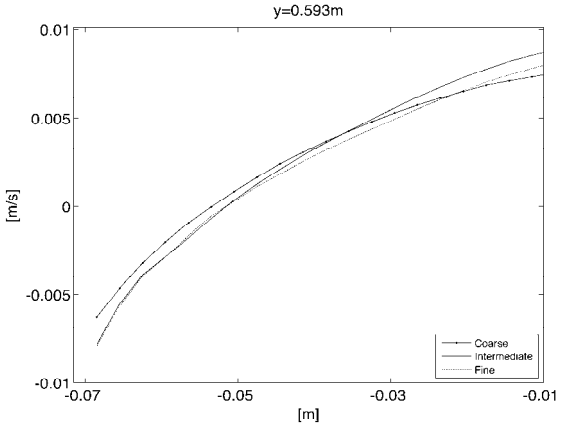

Figure 5: Mesh convergence - velocity profile after 45 minutes cool-down

The CFD simulations were run with a time step of maximum 1 s or a RMS CFL-number of 5, whichever was the most stringent.

RESULTS

The temperature excess ΔT with error bars is shown in Figure 6 and Figure 7 for all internal temperature sensors during three hours of cool-down. The comparisons show good agreement between the simulations (using the fine mesh) and experiments. Here the results from simulations with the *k-ω* model are shown together with the simulation without any turbulence model and the experimental data. The results show that there is good agreement between the CFD

simulations and the experimental data, but that the CFD simulations generally over estimates the temperature in the dead-leg region during both steady-state and cool-down.

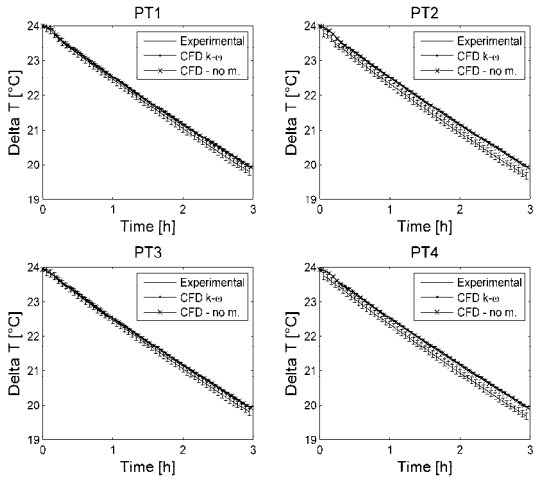

Figure 6: Experimental vs. CFD; PT1 - PT4 (internal sensors in the header)

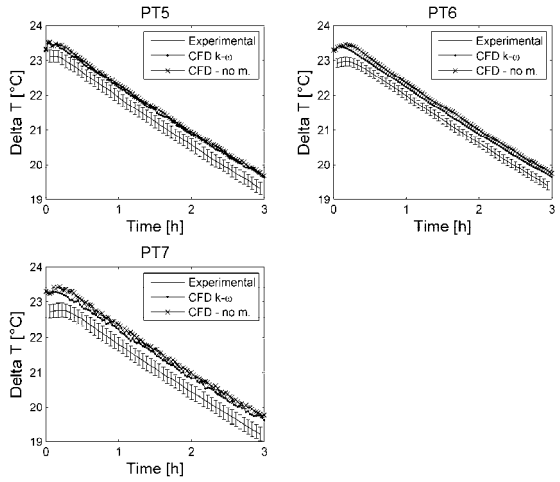

Figure 7: Experimental vs. CFD; PT5 - PT7 (internal sensors in the dead-leg)

A comparison between velocity profiles from CFD for the fine mesh and experiments are given in Figure 8 to Figure 10. Close to the wall in the dead-leg the production of turbulent kinetic energy is large, thus the flow is most likely fully turbulent here during the first part of the cool-down period. In the middle of the dead-leg, there is less mean shear; hence there is less production of turbulent kinetic energy. Turbulent kinetic energy is to some extent transported from the shear region to the middle of the pipe, but due to the limited amount of production the turbulence level in this region is smaller. As the insulated geometry cools down the driving force for the buoyant flow, the temperature excess ΔT, is smaller, hence the velocities also slow down. These two effects lead to a state where the flow close to the wall is turbulent, whereas the flow in the middle of the dead-leg is laminar. As mentioned earlier, this is a type of flow RANS-models cannot be expected to predict accurately.

After approximately two hours, see Figure 10, the production of turbulence in the shear zone is reduced and a laminar model is describing the velocity profiles better.

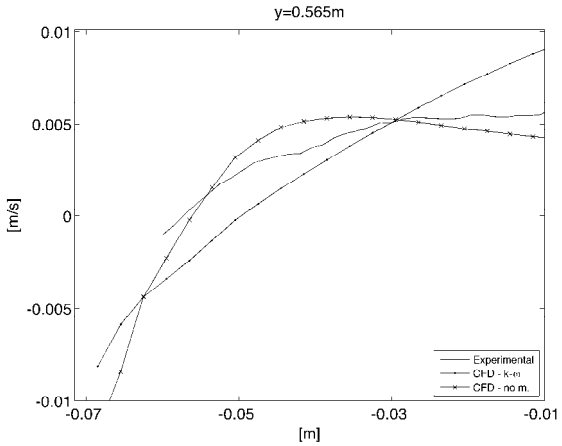

Figure 8: Vertical velocity at y=0.565m; CFD vs. exp - 15 min.

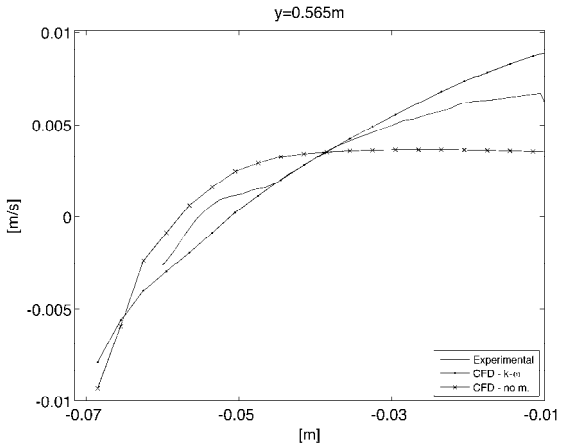

Figure 9: Vertical velocity at y=0.565m; CFD vs. exp - 60 min.

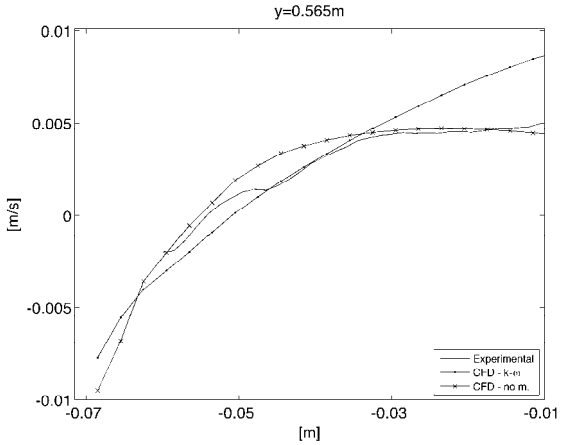

Figure 10: Vertical velocity at y=0.565; CFD vs. exp - 135 min.

Results from simulations with various turbulence models are shown in Figure 11 and Figure 12. The fine mesh was chosen and from the figures it is clear that the choice of model is important for accurate prediction of the velocity. The results show that there is virtually no difference between the *k*-ω, SST, and RSM-ω models in this case. Even though the RSM-ω model includes more physics compared to the two other models, it does not

predict the velocity field better than the simpler two-equation models.

As previously shown, the *k-ω* model compares satisfactorily with the tests for the first 100 minutes of the cool-down close to the wall. However, when the flow is laminar the *k-ω* fails in reproducing the velocity profiles. Then, a laminar model can be used. It can be seen from the results that the *k-ε* fails at all times. The reason for this is because this model uses wall functions, and then the near wall physics is not resolved nor accurately predicted. A RANS turbulence model that is able to simulate accurately the whole time period is not available. In this case, more sophisticated methods of treating turbulence are required, such as Direct Numerical Simulations (DNS) or Large Eddy Simulation (LES). LES with dynamic models such as the dynamic Smagorinsky-model have the prerequisite to predict this type of flow better than RANS-models. However, LES comes with a highly elevated computational cost compared to the RANS-simulations.

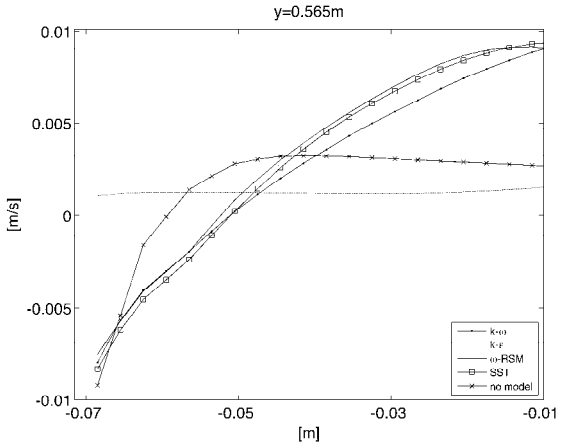

Figure 11: Mean velocity at y=0.565m for different numerical models. The x-axis denotes the horizontal position in the dead-leg - 30min.

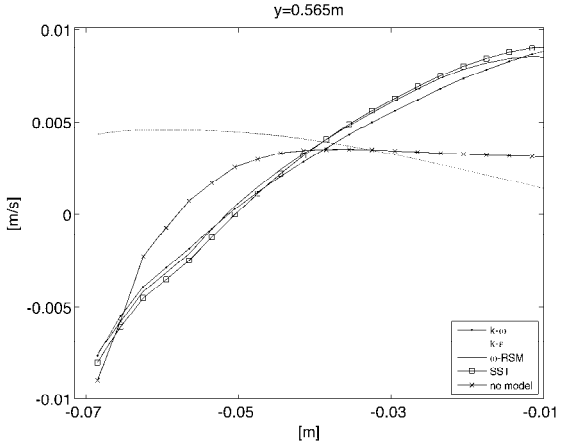

Figure 12: Mean velocity at y=0.565m for different numerical models. The x-axis denotes the horizontal position in the dead-leg - 120min.

CONCLUSION

A thorough comparison between results from CFD simulations and experimental tests of a simplified geometry resembling actual subsea equipment cool-down is conducted.

The choice of turbulence models and mesh refinement is discussed.

There are large discrepancies between results from the different turbulence models and also when the mesh size is varied. However, the results of the velocity profiles from *k-ω*, *ω-RSM* and *SST* are almost identical. The results clearly show the inadequacy of the often used standard of *k-ε* model for such problems. The reason for this is that the standard *k-ε* model uses wall functions that approximate the near wall physics which again is used to compute the wall shear and wall heat flux.

Even though the turbulence generated by buoyancy is anisotropic the results show that for this type of simulations an isotropic turbulence model can be used, e.g. the *k-ω* turbulence model. The anisotropy is weak compared to other effects. Furthermore the results show that in this case the Boussinesq-approximation may be used, the enforced equilibrium between Reynolds stresses and mean shear does not introduce any additional errors.

A mesh convergence test was carried out to determine the mesh level required for such type of geometries. The velocity fields proved rather insensitive to the mesh test, but the effect was clearly seen on the temperature field, particularly on the wall temperatures. It is concluded that when CFD simulations of subsea equipment cool-down are carried out, it is more important to conduct simulations on a proper mesh compared to choosing sophisticated turbulence models. (This is contradictory to what is often done in engineering, it is quicker and easier to change turbulence model rather than to re-mesh the model).

For this case the overall goal is to be able to estimate the temperature during cool-down. The choice of turbulence model is less important, but the quality and size of the mesh should get most of the attention.

Based on visual observations and a comparison between the CFD and experimental data it is concluded that the flow field after about 60 minutes is laminar, particularly in the middle of the dead-leg. Hence, no turbulence model should be used to predict the flow. However, in real life, for design simulations of thermal insulation on subsea equipment the actual flow field inside the geometries during a cool-down is unknown. One may make an estimate based on the expected Rayleigh number, but in practice, it is very difficult to accurately determine the type of flow. The CFD simulations have shown that the thermal field is generally insensitive to choice of turbulence models vs. no-model for this type of geometry. Hence, if it is uncertain whether the flow is turbulent or laminar, a turbulent simulation using the *k-ω* model will most likely produce adequate results for insulated equipment.

The results presented in this report are performed for the given pipe dimensions and flow rates. These results are not easily scalable, but methodology and mesh strategy are valid and carefully investigated and may be used for simulations of subsea equipment.

REFERENCES

AARNES, K.A., LESGENT, J. and HÜBERT, J.C., (2005), "Thermal Design of a Dalia SPS Deepwater Christmas Tree – Verified by Use of Full-Scale Testing and Numerical Simulations", *Offshore Technology Conference*, Houston, Texas, USA.

ASTERIADOU, K., HASTINGS, A.P.M., BIRD, M.R. and MELROSE, J., (2009), "Exploring CFD Solutions for Coexisting Flow Regimes in a T-Piece", *Chem. Eng. Technol*,, **32**, 948-955.

HABIB, M.A., BADR, H.M., SAID, S.A.M., MOKHEIMER, E.M.A., HUSSAINI, I. and AL-SANAA, M., (2005), "Characteristics of flow field and water concentration in a horizontal deadleg", *Heat and Mass Transfer*, **41**, 315-326.

BARAKOS, G. and MITSOULIS, E., (1994), "Natural convection flow in a square cavity Revisited: laminar and turbulent models with Wall functions", *International Journal for Numerical Methods in Fluids*, **18**, 695-719.

INCROPERA, F.P., DEWITT, D.P., BERGMAN, T.L. and LAVINE, A.S, (2007), "*Fundamentals of Heat and Mass Transfer* (6th ed.)", Hoboken: John Wiley & Sons.

LU, Y., MAROTTA, E. and SKEELS, B., (2011), "CFD Thermal Analysis of Subsea Equipment and Experimental Validation ", *Offshore Technology Conference, Houston, Texas, USA.*

MME, U., JOHANSEN, S.T., SARKAR, S., MOE, R., GOLDZAL, A. and LADAM, Y., (2008), "Flow and heat transfer in pipe caused by localised cold spot", *Progress in Computational Fluid Dynamics*, **9**, 409-416.

MOE, R., SØRBYE, S., SKOGEN, K. and LOFSEIK, C., (2005), "A comparison of experimental data and CFD predicted cool down in subsea equipment", *Fourth International Conference on CFD in the Oil and Gas, Metallurgical & Process Industries*, Tronheim, Norway, 6-8 June.

TAXY, S., and LEBRETON, E., (2004), "Use of Computational Fluid Dynamics to Investigate the Impact of Cold Spots on Subsea Insulation Performance", *Offshore Technology Conference*, Houston, Texas, USA.